

## Intelligent hybrid controlled structures with soil-structure interaction

X.Z. Zhang<sup>†</sup> and F.Y. Cheng<sup>‡</sup>

*Civil Engineering Department, University of Missouri-Rolla, Rolla, Missouri 65409, USA*

M.L. Lou<sup>‡†</sup>

*Institute of Structural Engineering & Disaster Reduction, Tongji University, Shanghai, 200092, China*

*(Received January 15, 2003, Accepted March 25, 2003)*

**Abstract.** A hybrid control system is presented for seismic-resistant building structures with and without soil-structure interaction (SSI). The hybrid control is a damper-actuator-bracing control system composed of passive and active controllers. An intelligent algorithm is developed for the hybrid system, in which the passive damper is designed for minor and moderate earthquakes and the active control is designed to activate when the structural response is greater than a given threshold quantity. Thus, the external energy for active controller can be optimally utilized. In the control of a multistory building, the controller placement is determined by evaluating the optimal location index (OLI) calculated from six earthquake sources. In the study, the soil-structure interaction is considered both in frequency domain and time domain analyses. It is found that the interaction can significantly affect the control effectiveness. In the hybrid control algorithm with intelligent strategy, the working stages of passive and active controllers can be different for a building with and without considering SSI. Thus SSI is essential to be included in predicting the response history of a controlled structure.

**Key words:** hybrid control; soil-structure interaction; intelligent control; shallow foundation; optimal location.

---

### 1. Introduction

Structural control implies that performance and serviceability of a structure are controlled to maintain prescribed limits during the application of environmental loads. Structural control is achieved in several ways: with passive or active control devices or with semiactive or hybrid systems. Passive devices utilize the fact that energy-dissipating mechanisms can be activated by the motion of structure itself. Active control devices require external energy for their operation. Semi-active devices are based on a passive device and improved by installing certain performance-adjusting functions such as semi-active stiffness, and semi-active vibration absorbers.

---

<sup>†</sup> Ph.D. Candidate

<sup>‡</sup> Curators' Professor Emeritus

<sup>‡†</sup> Professor

In order to gain the advantages of both passive and active devices, hybrid systems have recently been developed. The paper presents a hybrid damper-actuator bracing system. The system is based on a tube fluid damper (passive device) with an active controlled piston mounted on a structural brace. Passive, active and hybrid devices can be separately installed at different floors in order to provide both economical and effective control for a structure. Studies showed that for controlling the same amount of allowable displacement of a structure, the active control force for a hybrid control system can be significantly reduced in comparison with that due to active controller only. The hybrid control is further developed as an intelligent hybrid control system in which active controller begins to operate once maximum structural response exceeds a threshold value, and is adjusted if the response again over cross the second threshold value. To apply the control on a multi-story building, the optimal control location is an important issue which should be taken into account. Therefore the optimal location index (OLI) method is employed and discussed in this paper.

Most studies of control of seismic-resistant structures were based on the assumption that structures are fix-supported. This assumption is valid when structures are build on a rock or are not subjected to ground motion such as wind forces or mechanical vibration. This paper also presents the SSI effects. Both time and frequency domains are considered in the analysis. The results show that the consideration of SSI can cause control effectiveness reduction in structural response. In addition, SSI is also considered in the application of intelligent control algorithm.

## 2. Hybrid control system

### 2.1 Control devices and mechanics

The hybrid control system is composed of a viscoelastic damper as the passive part and a hydraulic actuator as the active part. They are mounted on a K-brace and connected with the building floor as illustrated in Fig. 1. There, cylinders of the damper and actuator are connected with the building floor and the piston bar of both is welded with the brace. Then,  $\Delta(t) = x_1(t) - x_b(t)$  is the motion difference between floor,  $x_1(t)$ , and brace,  $x_b(t)$ , which is the relative piston movement of the damper and actuator pistons.

The dynamic behavior of the damper follows the constitutive relationship of viscoelastic fluids may described by Maxwell Model (Cheng *et al.* 1996, Cheng *et al.* 1998) as

$$\lambda_0 \dot{f}_p(t) + f_p(t) = C_0 \dot{\Delta}_p(t) \quad (1)$$

where  $f_p(t)$  and  $\Delta_p(t)$  are the force on the damper and piston displacement, respectively.  $C_0$  is the passive damping coefficient and  $\lambda_0$  is the relaxation time.

The hydraulic actuator system consists of three components: an actuator, a servo-valve and a fluid pumping system (Cheng *et al.* 1996, Cheng *et al.* 1998). The servo-valve is described as first order dynamic system:

$$\tau \dot{c}(t) + c(t) = u(t) \quad (2)$$

where  $u(t)$  is control command and  $c(t)$  represents servo-valve piston displacements;  $\tau = 1/(2\pi f_b)$  and  $f_b$  is servo-valve bandwidth.

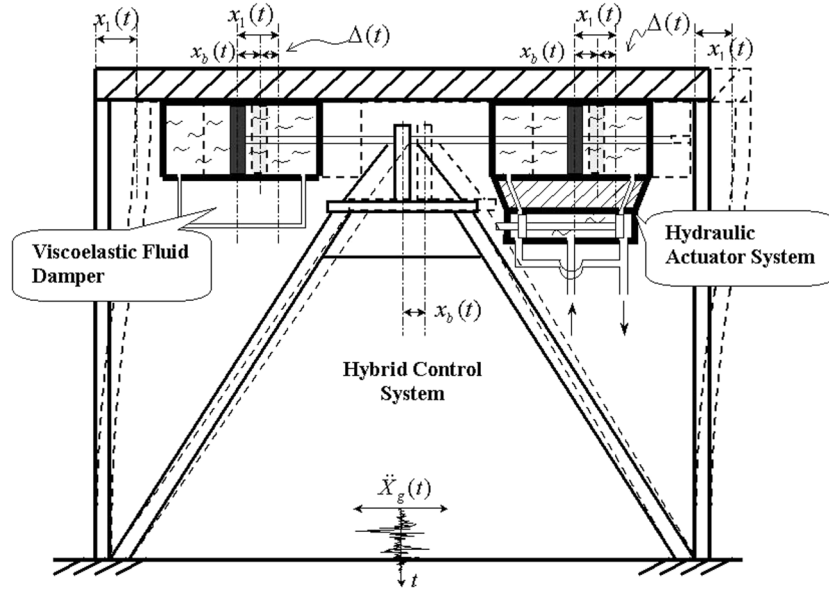


Fig. 1 Hybrid control system layout

The actuator is modeled as

$$\dot{f}_a(t) = \left( \frac{2\beta A^2}{V} \right) \dot{\Delta}_a(t) + \left( \frac{\beta A K_v}{V} \sqrt{2P_s} \right) c(t) \quad (3)$$

where  $f_a(t)$  and  $\Delta_a(t)$  are the active force supplied and actuator piston displacement, respectively.  $P_s$  is the fluids input pressure, which is generated by the pumping system and supposed to be a constant.  $A$ ,  $V$ ,  $\beta$  and  $K_v$  are actuator cylinder cross-section area, half cylinder volume, fluid bulk modulus and servo-valve pressure loss coefficient, respectively.

## 2.2 Intelligent control algorithms

The hybrid control system is targeted for using advantages of both passive and active control so that the external energy could be saved. The intelligent control strategy is developed for this hybrid system with three controlling stages, which are based on selected threshold values of an important structural response. Whenever the response exceeds one of the threshold values, the control system will be adjusted from the lower control stage to the next one. Under this control, the system is only under passive control for the small and moderate earthquakes if ever the response is smaller than the 1<sup>st</sup> threshold value, which is called control stage 1. Whenever the response exceeds the 1<sup>st</sup> threshold value, the active system is triggered and control system is in the control stage 2, in which both active and passive controls are working. The control stage 3 is designed to generate higher magnitude active force to resist stronger vibration when the structure response exceeds the 2<sup>nd</sup> threshold value.

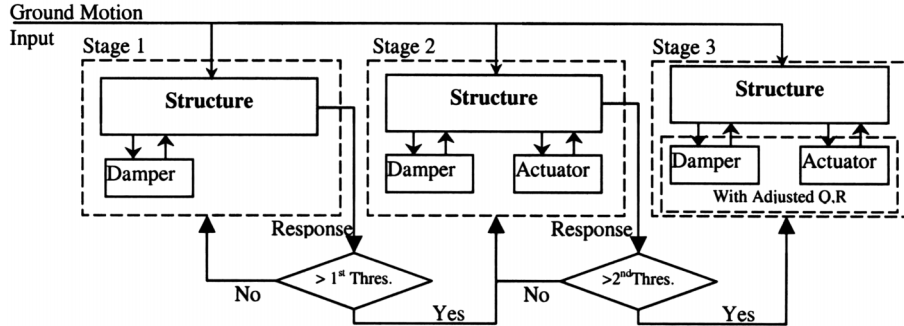


Fig. 2 Intelligent control strategy flow chart

Fig. 2 gives the flowchart of intelligent control strategy and it could be explained by the working procedure as:

1. Determine which structural response is the most important and set two thresholds for that.
2. The system in stage 1 for small and moderate earthquakes which cause a lower response than the first threshold.
3. The actuator starts to work whenever the response exceeds the first threshold values and the system gets into stage 2.
4. The system moves from stage 2 to stage 3 when the response exceeds the second threshold value. The weighting matrix value is adjusted and high active force is generated.

To execute the active control, the control command needs to be real-time supplied. For the requirement of the intelligent control, the control algorithms need to supply an increasing peak active force by adjust some control parameter, so that the proper parameter could then be set for control stage 2 and control stage 3 to yield real-time control command. The splitting-weighting control algorithm (Zhang *et al.* 2002) is used. The state space representations for structural system and controller system are modeled separately. For a general building structure with earthquake excitation and hybrid control force protection, its state space representation is

$$\{\dot{x}\} = [A_s]\{x\} + [B_{fa}]\{f_a(t)\} + [B_{fp}]\{f_p(t)\} + \{B_g\}\ddot{x}_g(t) \tag{4}$$

where  $[B_{fa}]$ ,  $[B_{fp}]$ ,  $\{B_g\}$  is the input location matrix for active force, passive force and ground acceleration, respectively;  $[A_s]$  is the system matrix for structure and  $\{x\}$  is the structural state vector. State representation for hybrid controller system can be obtained by combining Eqs. (1), (2) and (3) as

$$\{\dot{z}\} = [A_c]\{z\} + \{B_x\}\dot{\Delta}t + \{B_u\}u(t) \tag{5}$$

where  $\{z\} = [f_a \ f_p \ c]^T$  is the controller state vector, and  $[A_c]$  is the system matrix for the controller system;  $\{B_x\}$ ,  $\{B_u\}$  are the input matrices for the piston movement and control command, respectively. In the controller system, LQR technique can be employed to determine the control command,  $u$ , with the established fact that  $\dot{\Delta}$  can be treated as white noise stochastic process. The control command is obtained when controller feedback state and LQR feedback gain are observed or calculated. In such a way, an increasing maximum value for the active force can be yielded when

the weighting matrix of Q and R is changing as shown later in Fig. 5. Then the algorithms supplied an adjusting weighting matrix value to generate higher active force, which is needed in the intelligent control strategy for higher control stage.

### 3. Soil-structure interaction (SSI) formulation

For SSI, there are inertial interaction and kinematic interaction. The inertial interaction is much more significant than the kinematic interaction for shallow foundation. Thus the foundation-soil interaction stiffness and damping characteristics are quantified by impedance function for this study.

#### 3.1 Frequency domain analysis

Fig. 3 illustrates how soil-structure interaction is considered in the hybrid controlled building structure. For the SDOF building structure under ground acceleration input without control, the transfer function  $X_1(s)/\ddot{X}_g(s)$  could be expressed (Luco 1998, Smith *et al.* 1994) as

$$\frac{X_1(s)}{\ddot{X}_g(s)} = H(s)S(s) \tag{6}$$

where

$$H(s) = 1/(s^2 + 2\xi\omega_0s + \omega_0^2) \tag{7}$$

$$S(s) = \frac{-K_{HH}[I_Ts^2 + K_{MM}]}{mI_Ts^4 + (I_T + mK_{MM} + mh^2K_{HH})s^2 + K_{HH}K_{MM} - H(s)[mI_Ts^6 + (mK_{MM} + mh^2K_{HH})s^4]} \tag{8}$$

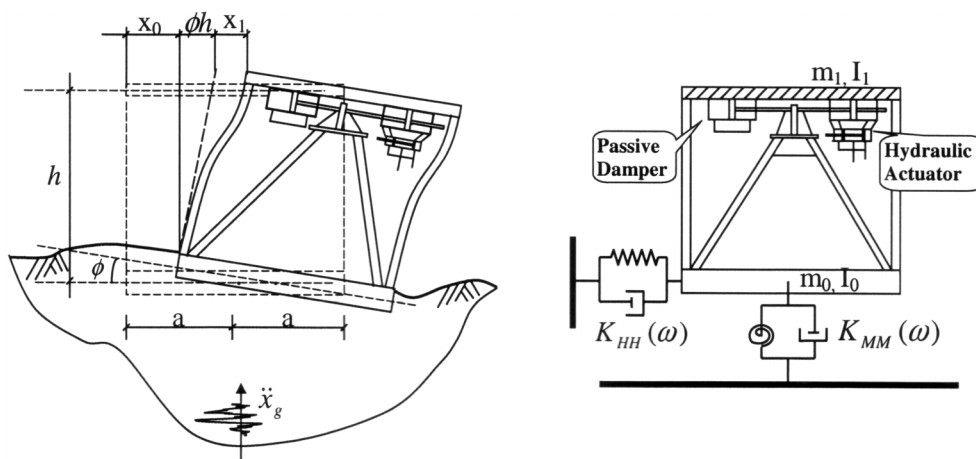


Fig. 3 SSI system with control and shallow foundation

where the variables are shown in Fig. 3 and  $I_T$  is the sum moment of inertia of structure and foundation. For the passive controlled SSI system, the transfer function  $X_1(s)/\ddot{X}_g(s)$  is derived as

$$\frac{X_1(s)}{\ddot{X}_g(s)} = H_p(s)S_p(s) \quad (9)$$

where

$$H_p(s) = (\lambda_0 s + 1)/((\lambda_0 s + 1)(s^2 + 2\xi\omega_0 s + \omega_0^2) + 2\xi\omega_0 s) \quad (10)$$

and  $S_p(s)$  is same as  $S(s)$  except for  $H(s)$ , which should be replaced by  $H_p(s)$  in Eq. (10).

The transfer function  $X_1(s)/\ddot{X}_g(s)$  for the hybrid-controlled system is also similarly derived as

$$\frac{X_1(s)}{\ddot{X}_g(s)} = H_{hf}(s)S_{hf}(s) \quad (11)$$

where

$$H_{hf}(s) = 1/(s^2 + 2\xi\omega_0 s + \omega_0^2 + 2\xi\omega_0 s/(\lambda_0 s + 1) + \alpha_1(\tau s^2 + s)/(\tau s^2 + s + \alpha_2 G_f)) \quad (12)$$

and  $S_{hf}(s)$  is same as  $S(s)$  except for  $H(s)$ , which should be replaced by Eq. (12);  $\alpha_1 = 2\beta A^2/V$ ,  $\alpha_2 = (\beta A K_{v\sqrt{2P_s}})/V$  and  $G_f$  is the force feedback gain.

### 3.2 Time domain analysis

The inertial interaction between soil and structure of the shallow foundation can be modeled by a set of frequency-independent springs and dashpots. Their stiffness and damping coefficients, denoted as  $K_s$  and  $C_s$ , equal to the corresponding impedance function items evaluated at the fundamental frequency of the SSI system (Wolf 1987). The motion equation for the hybrid controlled SSI system (for an  $n$ -story shear building) can be:

$$\begin{aligned} \begin{bmatrix} M_{\text{sup}} & 0 \\ 0 & M_f \end{bmatrix} \begin{Bmatrix} \ddot{X} \\ \ddot{X}_f \end{Bmatrix} + \begin{bmatrix} C_{\text{sup}} & -C_{\text{sup}}\Gamma \\ -\Gamma^T C_{\text{sup}} & \Gamma^T C_{\text{sup}}\Gamma + C_s \end{bmatrix} \begin{Bmatrix} \dot{X} \\ \dot{X}_f \end{Bmatrix} + \begin{bmatrix} K_{\text{sup}} & -K_{\text{sup}}\Gamma \\ -\Gamma^T K_{\text{sup}} & \Gamma^T K_{\text{sup}}\Gamma + K_s \end{bmatrix} \begin{Bmatrix} X \\ X_f \end{Bmatrix} \\ = \begin{bmatrix} -\gamma_a \\ \Gamma^T \gamma_a \end{bmatrix} \{f_a\} - \begin{bmatrix} -\gamma_p \\ \Gamma^T \gamma_p \end{bmatrix} \{f_p\} - \begin{bmatrix} M_{\text{sup}} & 0 \\ 0 & M_f \end{bmatrix} \begin{bmatrix} \Gamma \\ I_2 \end{bmatrix} \begin{Bmatrix} \ddot{x}_g \\ \ddot{\phi}_g \end{Bmatrix} \end{aligned} \quad (13)$$

where  $\Gamma = \begin{bmatrix} 1 & \dots & 1 & 1 & \dots & 1 \\ h_1 & \dots & h_n & h_{1b} & \dots & h_{1b} \end{bmatrix}^T$  to supply the information about floor and brace height.  $\{X\} =$

$\{x\} + [\Gamma]\{X_f\} = [x_1 \ x_2 \ \dots \ x_n \ x_{1b} \ x_{2b} \ \dots \ x_{nb}]^T + [\Gamma] \begin{Bmatrix} x_0 \\ \phi \end{Bmatrix}$ , where  $x_i$  is the  $i^{\text{th}}$  floor displacement,  $x_{ib}$  is

$i^{\text{th}}$  brace displacement and  $x_0$ ,  $\phi$  are foundation horizontal displacement and rotation, respectively.  $M_{\text{sup}}$ ,  $C_{\text{sup}}$ ,  $K_{\text{sup}}$  are super-structure (including braces) mass, damping and stiffness matrices.  $M_f =$

$\begin{bmatrix} m_0 & 0 \\ 0 & I_0 \end{bmatrix}$  and  $m_0, I_0$  are foundation mass and mass moment of inertia, respectively.  $\{f_a\}$  and  $\{f_p\}$  are active force and passive force input  $n$ -vector. The controllers' location is considered by the vector  $\gamma_a$  and  $\gamma_p$  in the equation. The whole system is input by the ground horizontal and rotational accelerations of  $\ddot{x}_g, \ddot{\phi}_g$ , and structural responses are calculated by matrix analysis (Cheng 2001).

#### 4. Optimal control location

For the control application on a multi-story building, there are a large number of controller placement combinations. Due to the significant affect on control's performance from the control placement, it is important to determine the optimal control location in order to maximally realize the control's function. The following optimal location index (OLI) (Pantelides and Cheng 1990)

$$\rho_b(x_i) = \sqrt{\sum_{j=1}^n \left\{ \frac{\Delta\phi_j(x_i)}{\Delta x_i} Y_j(T) \right\}^2} \quad (14)$$

is employed in this paper to determine the optimal control location. In Eq. (14), where  $x_i$  is the floor position, and  $n$  is the number of vibration modes considered based on fixed-support condition.  $\Delta\phi_j(x_i) = \phi_j(x_i) - \phi_j(x_{i-1})$  is the mode shape spatial difference from position  $x_i$  to  $x_{i-1}$ , and  $Y_j(T)$  is the spectrum value for the  $j^{\text{th}}$  mode. It is suggested that the control should be placed on the floor location with the larger calculated OLI. The definition of the OLI for the seismic structure reflects that an ideal location for the controller is where the displacement response of the uncontrolled structure is the largest.

### 5. Sample results

#### 5.1 One-story building

##### 5.1.1 Structural property

A one story building structure is selected to illustrate controlled response behavior. The floor mass is 1000 kg and column stiffness is  $1.097 \times 10^5$  N/m (period 0.6 sec. for the fixed-base condition). The impedance functions of the rigid footing on the half-space soil medium follow the model in Apsel *et al.* 1987. Both frequency and time domain analyses are conducted in this sample and intelligent control's applications with and without SSI are also discussed.

##### 5.1.2 Frequency domain analysis

The frequency domain analysis is executed for the uncontrolled, passive controlled and hybrid controlled building. The soil stiffness is changed by modifying its shear wave velocity. The floor frequency responses under the ground acceleration input for each system are drawn in plot as Fig. 4,

where,  $\eta(\text{dB}) = 20 \times \frac{|X_1|}{|\ddot{X}_g|}$  and soil becomes softer from case (1) through (3). The softer soil causes the

fundamental frequency reduced for both with control and w/o control cases. Also note that both passive and hybrid control effectiveness become less when the soil becomes softer.

More detailed results are listed in Table 1. There are 5 soil cases from very soft soil ( $V_s = 30$  m/s) to the fixed-base ( $V_s = \infty$ ) and the fundamental frequency of the structure (w/o control case) is

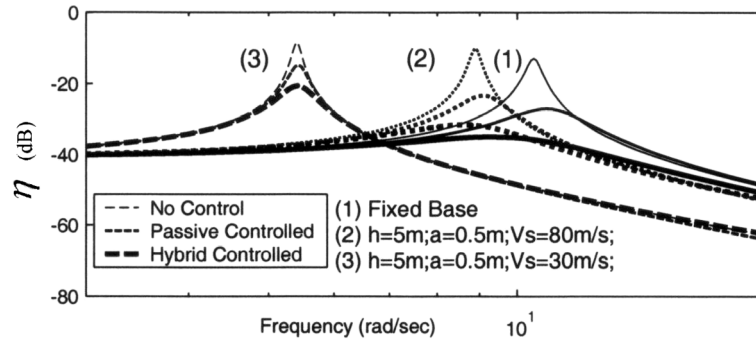


Fig. 4 Frequency responses

Table 1 Frequency vs peak value of  $|X_1(s)|/|\ddot{X}_g(s)|$  by changing  $V_s$

Control \ Response		SSI case	$V_s = \infty$	$V_s = 100$ m/s $a = 0.5$ m $h = 5$ m	$V_s = 80$ m/s $a = 0.5$ m $h = 5$ m	$V_s = 50$ m/s $a = 0.5$ m $h = 5$ m	$V_s = 30$ m/s $a = 0.5$ m $h = 5$ m
		W/O	(a) Peak $ X_1(s) / \ddot{X}_g(s) $ ( $\text{sec}^2$ )		0.229	0.292	0.316
Control	Freq. at peak (rad/s)		10.5	9.37	8.89	7.42	5.41
Passive Control	(b) Peak $ X_1(s) / \ddot{X}_g(s) $ ( $\text{sec}^2$ )		0.0447	0.0603	0.0692	0.1047	0.182
	Freq. at peak (rad/s)		10.9	9.63	9.22	7.52	5.43
	(b)/(a)		19.5%	20.6%	21.9%	28.1%	47.6%
Hybrid Control	(c) Peak $ X_1(s) / \ddot{X}_g(s) $ ( $\text{sec}^2$ )		0.0178	0.0232	0.0266	0.043	0.0923
	Freq. at peak (rad/s)		9.67	8.91	8.61	7.4	5.42
	(c)/(a)		7.77%	7.94%	8.4%	11.6%	24.16%

Table 2 Frequency vs peak value of  $|X_1(s)|/|\ddot{X}_g(s)|$  by changing  $a$

Control \ Response		SSI case	$V_s = \infty$	$V_s = 30$ m/s $a = 1$ m $h = 5$ m	$V_s = 30$ m/s $a = 0.8$ m $h = 5$ m	$V_s = 30$ m/s $a = 0.6$ m $h = 5$ m	$V_s = 30$ m/s $a = 0.5$ m $h = 5$ m
		W/O	(a) Peak $ X_1(s) / \ddot{X}_g(s) $ ( $\text{sec}^2$ )		0.229	0.1905	0.2113
Control	Freq. at peak (rad/s)		10.5	9.0	8.08	6.5	5.41
Passive Control	(b) Peak $ X_1(s) / \ddot{X}_g(s) $ ( $\text{sec}^2$ )		0.0447	0.0575	0.0733	0.1202	0.182
	Freq. at peak (rad/s)		10.9	9.19	8.20	6.54	5.43
	(b)/(a)		19.5%	30.2%	34.7%	42.2%	47.6%
Hybrid Control	(c) Peak $ X_1(s) / \ddot{X}_g(s) $ ( $\text{sec}^2$ )		0.0178	0.0245	0.032	0.0569	0.0923
	Freq. at peak (rad/s)		9.67	8.61	7.93	6.5	5.42
	(c)/(a)		7.77%	12.9%	15.1%	20.0%	24.16%

Table 3 Frequency vs peak value of  $|X_1(s)|/|\ddot{X}_g(s)|$  by changing  $h$

Control		SSI case		$V_s = \infty$	$V_s = 30$ m/s $a = 0.5$ m $h = 2$ m	$V_s = 30$ m/s $a = 0.5$ m $h = 3$ m	$V_s = 30$ m/s $a = 0.5$ m $h = 4$ m	$V_s = 30$ m/s $a = 0.5$ m $h = 5$ m
		Response						
W/O Control	(a) Peak $ X_1(s) / \ddot{X}_g(s) $ (sec <sup>2</sup> )			0.229	0.2512	0.2884	0.3323	0.382
	Freq. at peak (rad/s)			10.5	8.66	7.39	6.29	5.41
Passive Control	(b) Peak $ X_1(s) / \ddot{X}_g(s) $ (sec <sup>2</sup> )			0.0447	0.0684	0.0933	0.1349	0.182
	Freq. at peak (rad/s)			10.9	8.84	7.56	6.34	5.43
	(b)/(a)			19.5%	27.2%	32.4%	41.8%	47.6%
Hybrid Control	(c) Peak $ X_1(s) / \ddot{X}_g(s) $ (sec <sup>2</sup> )			0.0178	0.0275	0.0417	0.0631	0.0923
	Freq. at peak (rad/s)			9.67	8.42	7.35	6.3	5.42
	(c)/(a)			7.77%	10.9%	14.5%	19.0%	24.16%

reduced from 10.5 rad/s to 5.41 rad/s. The magnitude ratio  $|X_1(s)|/|\ddot{X}_g(s)|$  under passive control is changed from 0.0447 to 0.182 corresponding to  $V_s = \infty$  through  $V_s = 30$  m/s. For the hybrid controlled case, the magnitude ratio  $|X_1(s)|/|\ddot{X}_g(s)|$  varies from 0.0178 to 0.0923 associated with  $V_s = \infty$  through  $V_s = 30$  m/s. The change of magnitude ratio can be similarly observed when foundation dimension decreases for a given soil shear velocity and a given building height as shown in Table 2. The trend of magnitude ratio changes is given in Table 3 for the changing building height with a given  $V_s$  and a given foundation dimension.

### 5.1.3 Time domain analysis

For the time history analysis, the foundation is 4 m × 4 m square and the floor height is 10 m. The system is subjected to El Centro earthquake (NS component, 50% magnitude) input and protected by the hybrid control system. As shown in Table 4, there are four kinds of supporting conditions as fixed-base ( $V_s = \infty$ ) and three different soils ( $V_s = 150$  m/s, 80 m/s, and 50 m/s) considered. For each

Table 4 SSI influence on hybrid control effectiveness

Response		SSI Fixed-base	Soil Condition 1		Soil Condition 2		Soil Condition 3	
		$V_s = \infty$	$a = 2$ m; $h_1 = 10$ m; $V_s = 150$ m/s		$a = 2$ m; $h_1 = 10$ m; $V_s = 80$ m/s		$a = 2$ m; $h_1 = 10$ m; $V_s = 50$ m/s	
Control	$x_1$ (cm) (Ratio)	$x_1$ (cm) (Ratio)	$x_{ssi}$ (cm) (Ratio)	$x_1$ (cm) (Ratio)	$x_{ssi}$ (cm) (Ratio)	$x_1$ (cm) (Ratio)	$x_{ssi}$ (cm) (Ratio)	
W/O Control	4.20 (Ref. number)	4.18 (Ref. number)	4.20 (Ref. number)	4.11 (Ref. number)	4.19 (Ref. number)	3.98 (Ref. number)	4.16 (Ref. number)	
Control Case 1	2.16 (51.4%)	2.17 (51.8%)	2.18 (51.9%)	2.17 (52.8%)	2.22 (53.0%)	2.19 (54.9%)	2.30 (55.4%)	
Control Case 2	1.53 (36.4%)	1.54 (36.8%)	1.55 (36.9%)	1.55 (37.6%)	1.58 (37.8%)	1.57 (39.4%)	1.66 (39.9%)	
Control Case 3	0.71 (17.0%)	0.72 (17.2%)	0.73 (17.3%)	0.73 (17.8%)	0.75 (18.0%)	0.75 (18.9%)	0.82 (19.7%)	

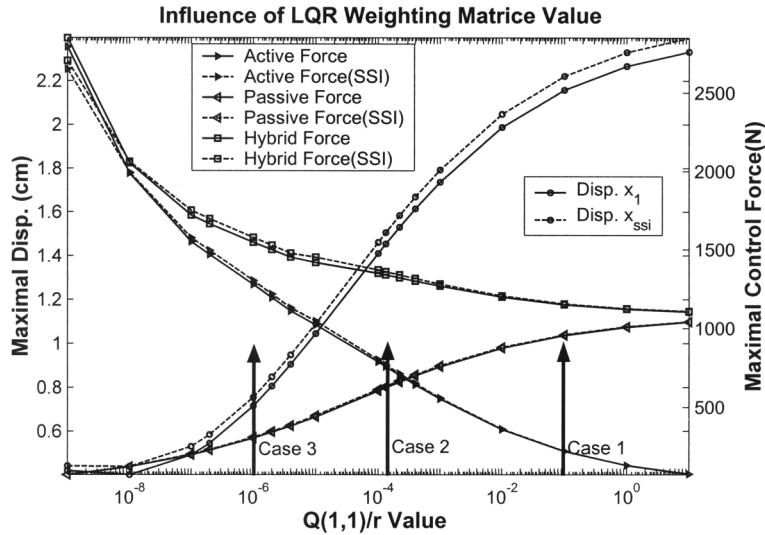


Fig. 5 SDOF control cases with and W/O SSI

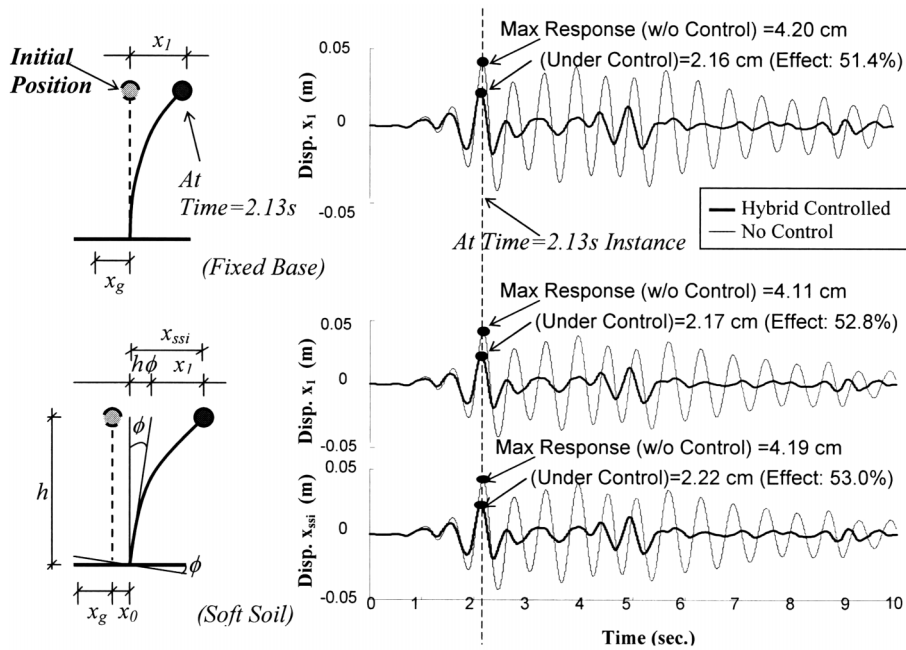


Fig. 6 Time history responses

supporting case, the floor response of  $x_1$  and  $x_{ssi}$  are listed for W/O control case and three control cases. Three control cases are based on three different  $Q(1,1)/R$  values to present three response ratios as demonstrated in Fig. 5. For instance, in soil condition 2 ( $V_s = 80$  m/s), the ratio between displacement with SSI and the displacement with SSI but W/O control is 52.8% when  $Q(1,1)/R$  is set as  $10^{-1}$ ; the same  $Q(1,1)/R$  is used to calculate the ratio between fixed-base displacement with

control and the displacement without control. Table 4 shows a complete ratio comparison, in which  $x_1$  is relative floor displacement and  $x_{ssi}$  is displacement between floor and column support as illustrated in Fig. 6. The uncontrolled response is set as a reference number and response ratio is the controlled displacement divided by the reference number as shown in the bracket for each case. For instance, in soil condition 2 ( $V_s = 80$  m/s) at control case 1, the displacement ratio of  $x_1$ (fixed-base) is 51.4%, which is smaller than the ratios in terms of either  $x_1$ (with soil), 52.8% or  $x_{ssi}$ , 53.0%, respectively. This can be observed from Fig. 6. It is apparent that the control effectiveness was reduced when the SSI is considered. If the other two soil conditions are also compared, the larger ratio may be observed when the soil becomes softer. Thus it can be concluded that the control effectiveness becomes less when the soil is softer as evidenced by both time history and frequency domain analyses.

5.1.4 Intelligent control with and without SSI

In this study, SSI influence is discussed when the intelligent control strategy is employed in the hybrid control’s application. The threshold quantities are assigned for the floor’s displacement response, which is  $x_1$  for fixed-base case and  $x_{ssi}$  for soil case. The first and second threshold values are set as 3.0 cm and 4.0 cm, respectively. Two cases of examples are supplied here with different input ground motion magnitude. One is El Centro Earthquake with the reduced magnitude as 62% of the original and the other is 95% in order to yield the response with SSI at stage 2 and stage 3, respectively.

Case 1. Sixty-two percentile (62%) magnitude El Centro

Two hybrid controlled systems are simulated in this case. One is fixed-base (System-1) and the other is supported on the soil with shear wave velocity of 80 m/s (System-2). In both systems, the intelligent control strategy guides hybrid control’s operation. Fig. 7 shows the displacement and force response time history of System-1. In the 10 second duration of vibration, the hybrid system keeps working in the stage 1 because the displacement (maximum 2.98 cm at point B and/or C) is

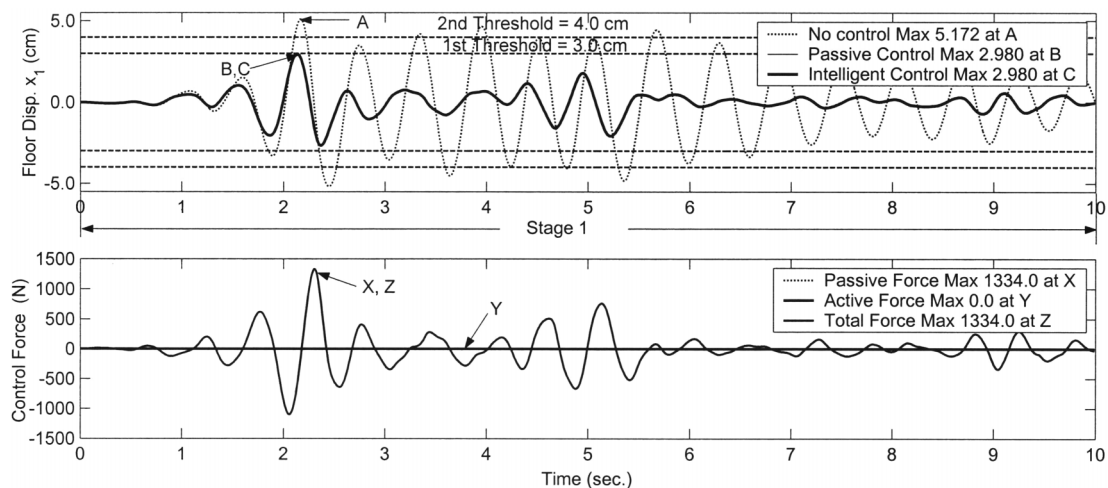


Fig. 7 Intelligent control under 62% El Centro (fixed-base)

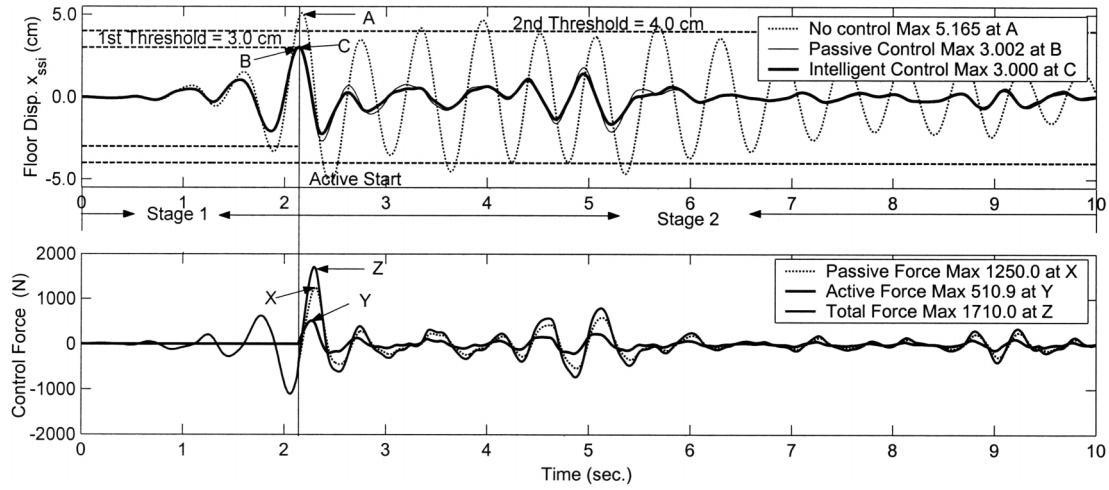


Fig. 8 Intelligent control under 62% El Centro (with soil)

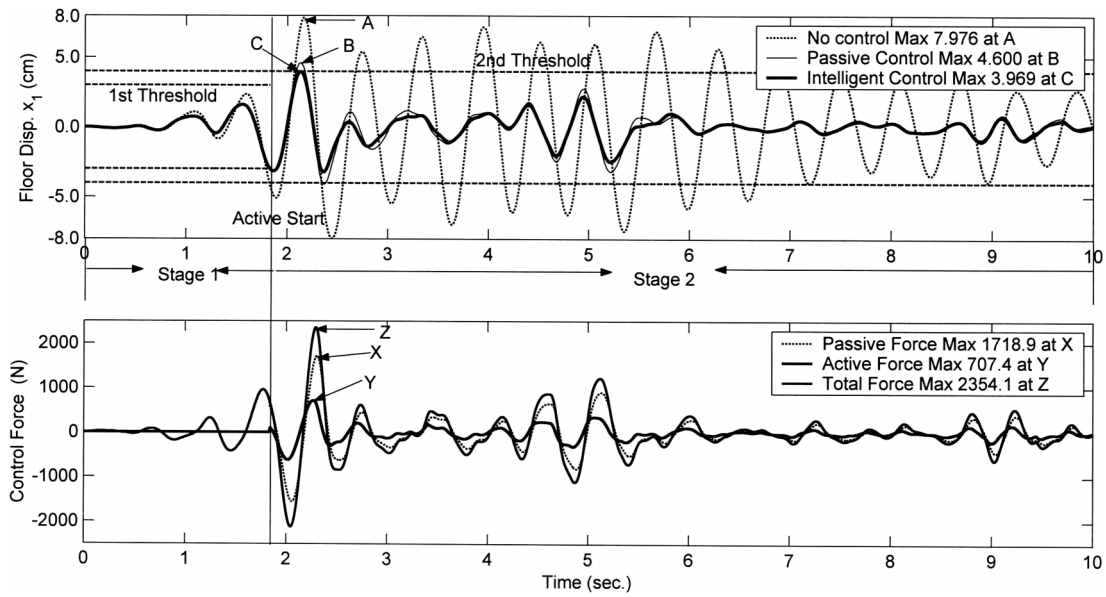


Fig. 9 Intelligent control under 95% El Centro (fixed-base)

always below the 1<sup>st</sup> threshold. But in the time history of System-2 as shown in Fig. 8, the response goes into stage 2 at 2.13s and the actuator begins to work. As to force response, in System-1, the active force is always zero and the passive force is the total force with the maximum value of 1334.0 N at point X and/or Z in Fig. 7; in System-2, active force is generated in stage 2 with maximum 510.9 N at point Y and maximum total force with 1710.0 N at point Z in Fig. 8.

The reason for two system's different process is due to the larger displacement response  $x_{ssi}$  (with soil) than  $x_1$  (fixed-base). It happens at the condition that  $x_1$  is below the 1<sup>st</sup> threshold value but  $x_{ssi}$  is over that value as in this case.

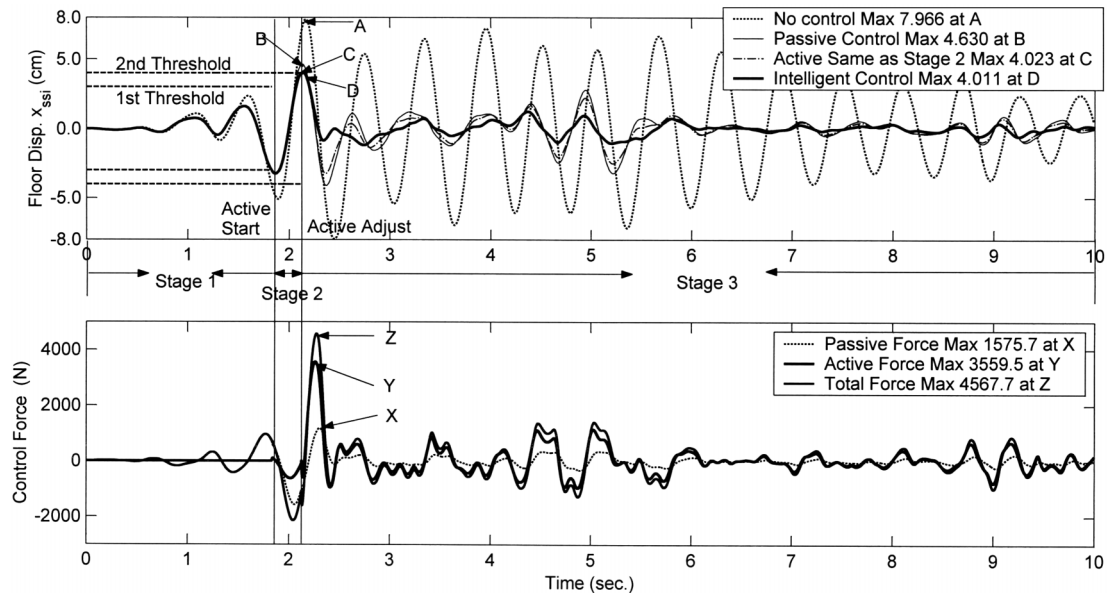


Fig. 10 Intelligent control under 95% El Centro (with soil)

#### Case 2. Ninety-five percentile (95%) magnitude El Centro

Fig. 9 is the response history of System-1 under the higher magnitude ground motion input. The response passes stage 1 and then reaches the stage 2 threshold at 1.81s. The actuator starts to work at that instant and its maximum peak value is 707.4 N at point Y. The passive and hybrid total forces have their maximum peak values of 1718.9 N and 2354.1 N at point X and Z, respectively.

For System-2, the response goes into stage 3 at 2.2s but System-1 doesn't because SSI is considered in former as shown in Fig. 10. When the System-2 is at stage 3, more weighting is set on the active system and then higher active force is generated. Therefore, the maximum active force and total hybrid force go up to 3559.5 N and 4567.7 N at point Y and Z, respectively. They consequently yield more reduction in displacement.

For the application of the intelligent strategy in the structural system with and without considering SSI, a different process appears in response history and control's operation. In case 1, actuator is operated in System-2 but never be used in System-1. In case 2, higher active force is generated at stage 3 and then more displacement is reduced for System-2 in comparison with the displacement and force response of System-1.

## 5.2 Three-story model building

### 5.2.1 Structural property

A three-story steel model building is employed in this example (Cheng *et al.* 1994). This model, 1/4 size of the full-scale structure, is 2.54 m high, 1.22 m long and 0.61 m wide. The floors' mass are 593.8 kg, 590.2 kg, and 576.6 kg, for the first, second and third floors, respectively. The structure has frequencies of 2.622, 9.008, and 17.457 cycle/s (note that the time scale factor is 1:2 and makes the natural frequency of a model two times as the prototype structure). The damping

ratios are 0.364%, 0.354% and 0.267% for the 3 modes, respectively. The K-brace stiffness is 1549 kN/m and the damping ratio is 0.1%.

### 5.2.2 Intelligent control without SSI

In the example, the top floor displacement is taken as most important response; first and second threshold values are set as 1.2 cm and 1.6 cm, respectively. The El Centro Earthquake record with time scale 1:2 is used as ground motion input. To demonstrate the different possible hybrid system working status, three cases of control process are given below with the increasing input ground accelerating magnitude.

#### Case 1. Fifty percentile (50%) magnitude of original El Centro record

In this case, the El Centro record magnitude is set as 50% of the original. In six seconds of response time history (Fig. 11), the control system keeps working in stage 1 because the controlled peak top-floor displacement is 1.05 cm ( $<$  first threshold). In this stage there is only passive damper working and the active force is always zero, shown in Fig. 13(b).

#### Case 2. Seventy-five percentile (75%) magnitude of original El Centro record

In Fig. 12, we can see the control system goes into stage 2 at 0.95 s and then keeps working in stage 2. In Fig. 12(b), the active force is zero before that time instant and with a peak value of 413.3 N in its whole working process. The passive control force's peak value is 1388.3 N, which is higher than the peak value of the active force. In intelligent control, we usually set a relatively smaller active force than the passive force in stage 2 and let passive system still take dominant rule in stage 2.

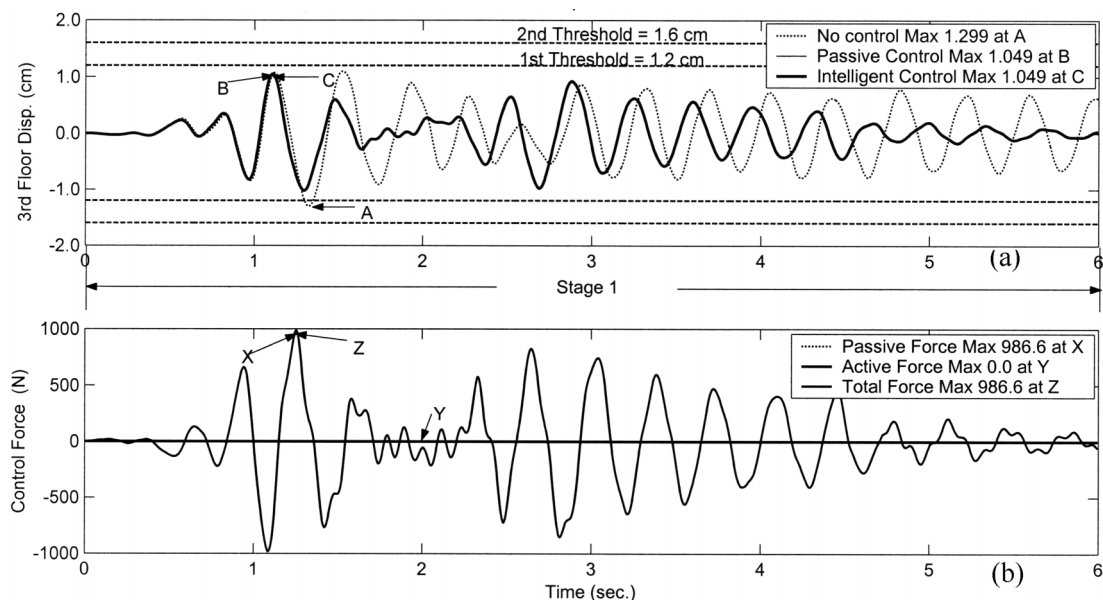


Fig. 11 Intelligent control results for Case 1 (a) Top floor displacement (b) Control force

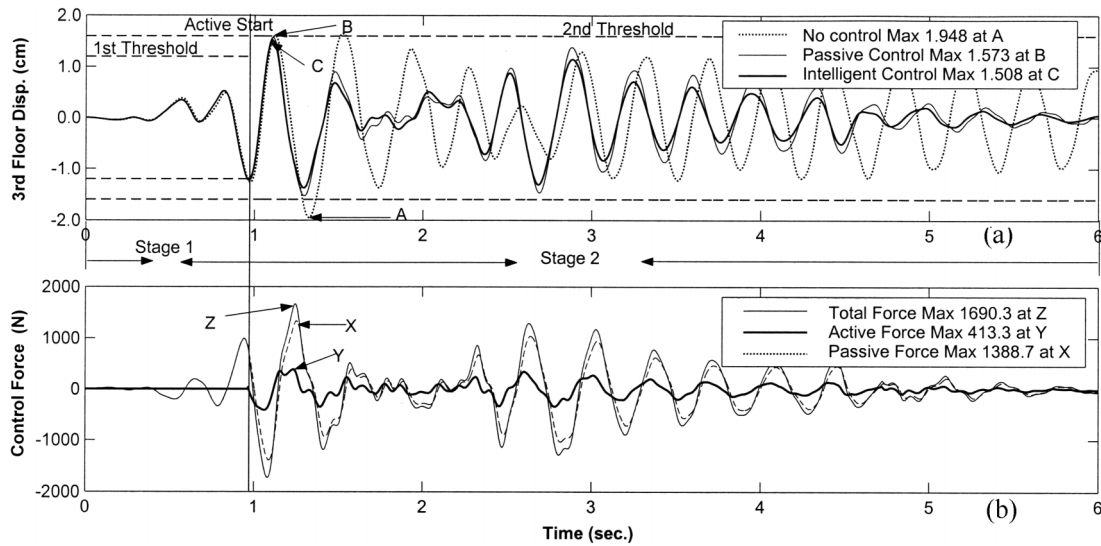


Fig. 12 Intelligent control results for Case 2 (a) Top floor displacement (b) Control force

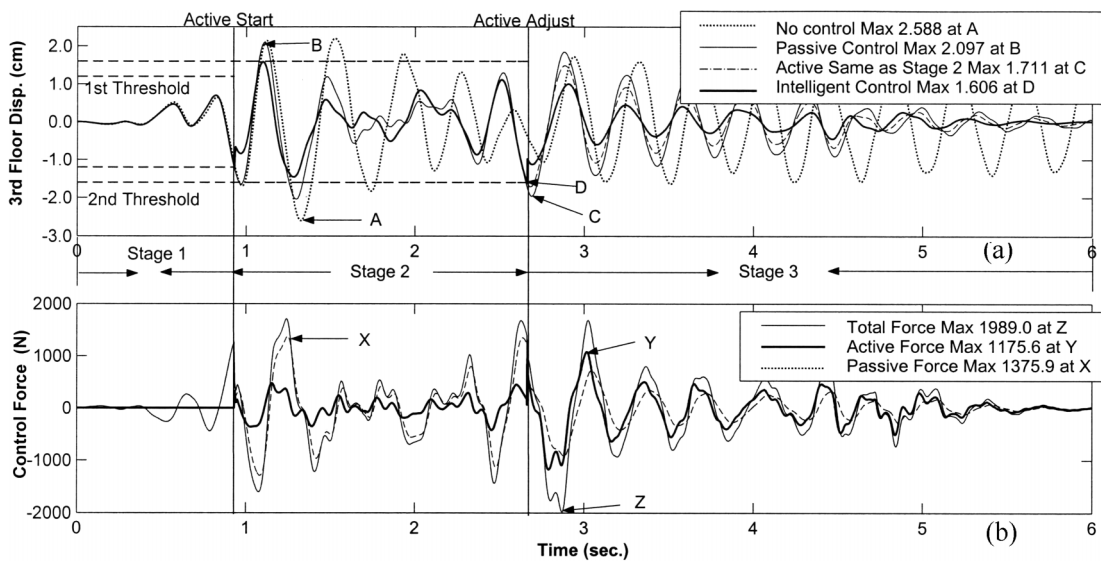


Fig. 13 Intelligent control results for Case 3 (a) Top floor displacement (b) Control force

Case 3. Hundred percentile (100%) magnitude of original El Centro record

The time history responses for this case are given in Fig. 13. The control system skipped from stage 1 into stage 2 at time 0.9 s due to the over-crossing of passive controlled response from the first threshold; and skipped from stage 2 into stage 3 at time instant 2.65 s, where the controlled response (in stage 2) exceeds the second threshold.

In Fig. 13(b), the active force is zero when the system is in the stage 1. In the second stage, passive force is with the peak value of 1375.88 N, which is larger than active force. When the

system gets into stage 3, relatively larger active force is generated than in stage 2 and its peak is 1175.56 N, which is larger than passive force in stage 3. Thus the intelligent control can sufficiently use passive part in lower stage and let the active part be dominant at higher response stage.

### 5.3 Ten-story building

#### 5.3.1 Structural property

The 10-story building has height, mass and column stiffness for each floor as 3.75 m,  $1.0 \times 10^4$  kg,  $1.0 \times 10^7$  N/m, respectively. Fundamental frequency is 4.73 rad/s. The damping ratios for the first four modes are assumed to be 2%. The foundation is 6 m  $\times$  6 m square with mass  $2 \times 10^4$  kg and mass moment of inertia  $6 \times 10^4$  kg-m<sup>2</sup>. The soil media has the following characteristics: Shear wave velocity = 150 m/s, shear modulus =  $4.5 \times 10^7$  N/m<sup>2</sup> and Poisson's ratio = 0.333. The impedance functions are based on Apsel *et al.* 1987.

#### 5.3.2 Determination of OLI for six earthquake sources

To decide where the hybrid control devices should be installed, OLI is calculated for this structure. The spectra of five different earthquake records, El Centro 1940, Kobe 1995, San Fernando 1971, Northridge 1994, artificial; along with Newmark design spectrum are employed. Spectral displacements  $Y_j(T)$  are shown in Fig. 14. The OLI values are illustrated in Fig. 15 and the two floors with higher OLI for each case are labeled as I and II. Note that the indices at the first and second floors are higher than other floors, which suggest that controllers should be installed on these floors.

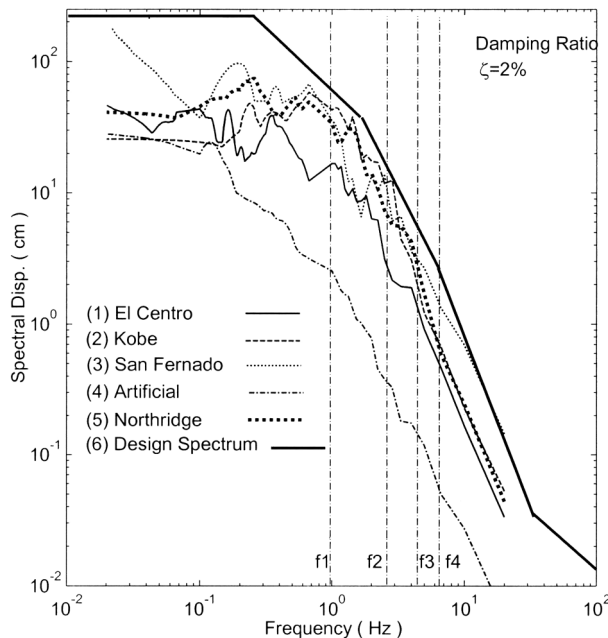


Fig. 14  $Y_j(T)$  for six earthquake spectra

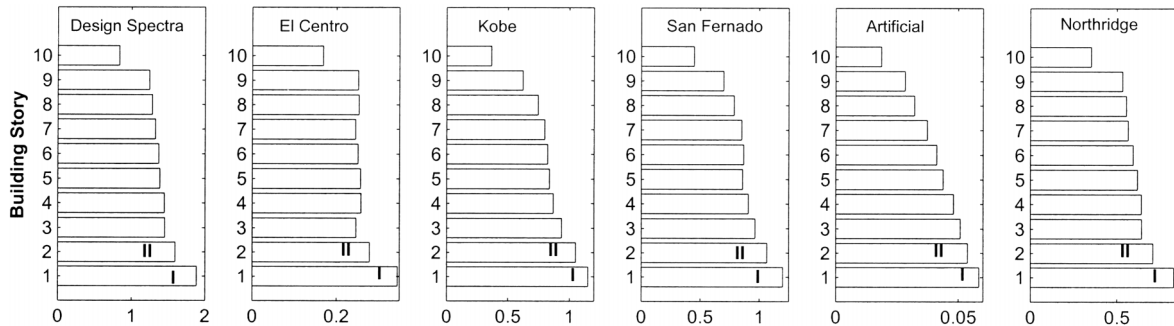


Fig. 15 Optimal location index (OLI)

### 5.3.3 Response comparison with and without SSI

In the time history analysis, both fixed-base and SSI cases are conducted with and without control. In Fig. 16, the  $Q(1,1)/r$  influence curves are illustrated. By setting the allowable displacement of the 10<sup>th</sup> floor as 13.5 cm,  $Q(1,1)/r$  values are then chosen for both fixed-base and SSI cases. The responses history of the 10<sup>th</sup> floor displacement and control force at the 1<sup>st</sup> floor for both cases are shown in Fig. 17, and Fig. 18 shows the foundation responses history with and without control, under the El Centro earthquake (NS component) input. The maximum displacement of the fixed-base case is smaller than that of the soil case (at point A and C in Fig. 17), which is due to the foundation rotation response with the maximum  $6.4 \times 10^{-4}$  rad at point X in Fig. 18. When 10<sup>th</sup> floor displacements of both cases are controlled to 13.5 cm as point B and D in Fig. 17, the fixed-base case needs maximum control force of  $4.2 \times 10^4$  N at the first floor (point X in Fig. 17), but  $5.7 \times 10^4$  N for the SSI case (point Y in Fig. 17). It needs higher control force for SSI system to yield the same maximum top floor displacement in comparison with the fixed-base system.

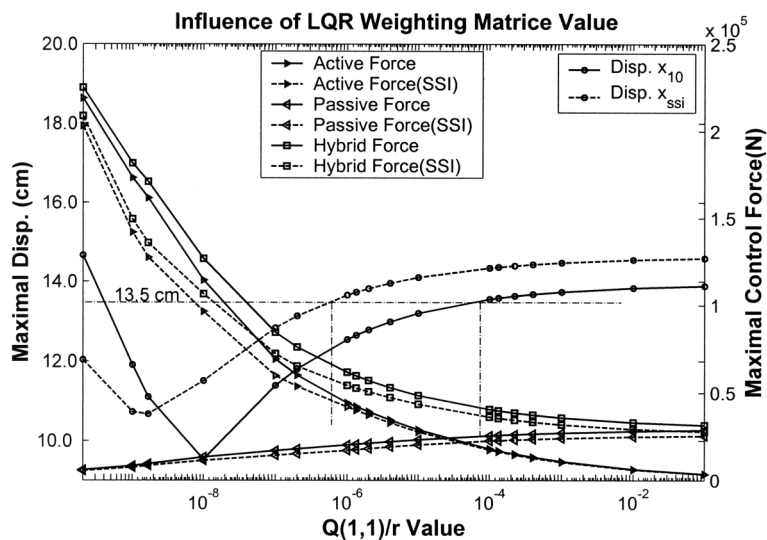


Fig. 16 Maximal control force and maximal reduced displacement

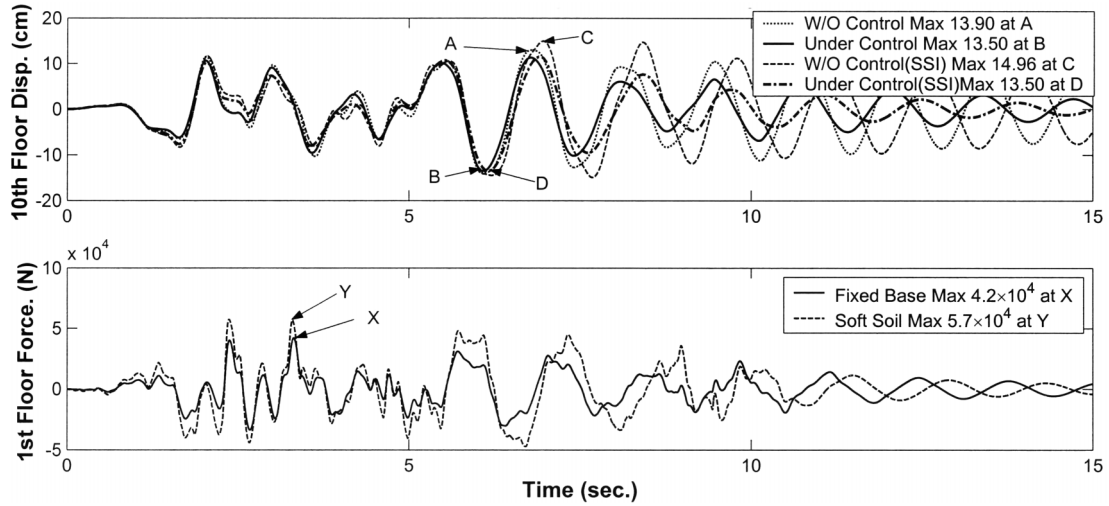


Fig. 17 Displacement and force responses for fixed-base and SSI

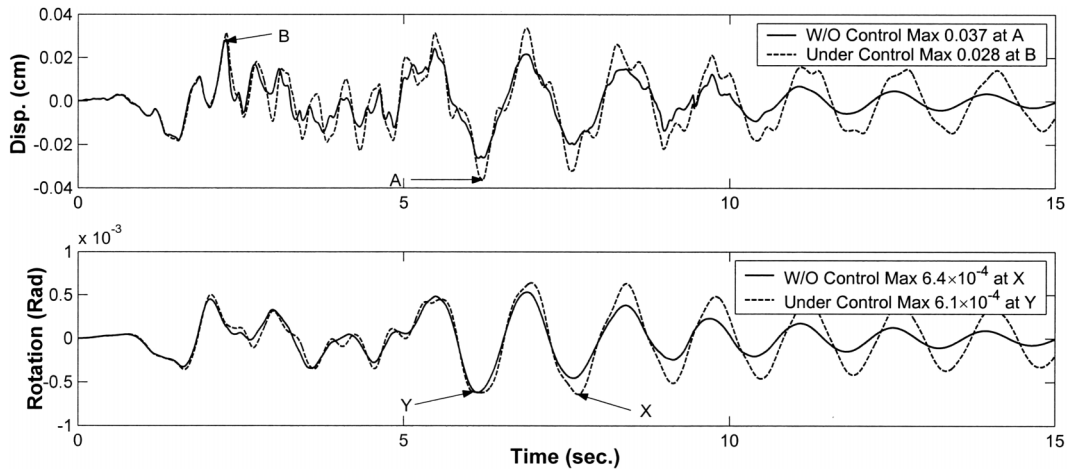


Fig. 18 Hybrid controlled foundation responses

**6. Conclusions**

- The hybrid control system with intelligent control strategy can significantly increase control effectiveness. The passive damper is designed for minor and moderate earthquakes and actuator begins to work when passive capacity could not satisfy the prescribed requirement under larger earthquakes. Thus both advantages of passive and active devices can be fully utilized and the external energy can be consequently saved.
- SSI can decrease control effectiveness. In comparison with fixed-base shallow-foundation case, when the soil becomes softer, both passive and hybrid control effects become less as shown in both frequency and time domain analyses. As reflected in the SDOF sample, the ratio of controlled displacement with the displacement of uncontrolled structure is 51.4% for fixed-base

case, but the ratio goes up to 53.0% when SSI is considered for both controlled and uncontrolled systems.

- Higher control force is needed for the building on soil than on the fixed-base to yield the same maximum displacement response. For instance, in time history analysis of the ten-story building,  $5.7 \times 10^4$  N of the first floor control force is needed to control 10<sup>th</sup> floor's displacement to 13.5 cm for SSI ( $V_s = 150$  m/s), but it only needs  $4.2 \times 10^4$  N if the structure is considered as fixed-base.
- Optimal location index (OLI) is a useful technique in determining controllers' placement for multi-story building as shown in the example presented.
- In order to achieve the control effectiveness of a structure, it is recommended to consider SSI and intelligent control strategy for properly predicting the working stages of passive and active controllers along with structural response history.

## Acknowledgements

Partial results presented herein are resulting from a US-China joint research project in collaboration with Tongji University, China, for which the US side is supported by the grant NSF CMS 9903136. The authors are grateful for the cooperation between UMR and Tongji as well as the financial support from both countries.

## References

- Apsel, R.J. and Luco, J.E. (1987), "Impedance functions for foundations embedded in a layered medium: an integral equation approach", *Earthq. Eng. Struct. Dyn.*, **15**, 213-231.
- Cheng, F.Y. and Tian, P. (1994), "Design parameter analysis of hybrid optimal controlled structures", *Proc. of 2<sup>nd</sup> Int. Conf. on Intelligent Materials (Ed. Craig A. Rogers and C.G. Wallace)*, Williamsburg, 340-351.
- Cheng, F.Y., Tian, P., Rao, V., Martin, K., Liou, F. and Yeh, J.H. (1996), "Theoretical and experimental studies on hybrid control of seismic structures", *Proc. of the 12<sup>th</sup> ASCE Conf. on Analysis and Computation (Ed. F.Y. Cheng)*, Chicago, 322-338.
- Cheng, F.Y. and Jiang, H.P. (1998), "Optimal control of a hybrid system for seismic excitations with state observer technique", *Journal of Smart Materials and Structures*, **7:5**, 654-663.
- Cheng, F.Y., Jiang, H.P. and Lou, M.L. (1999), "State-of-the-art of control systems and SSI effect on active control structures with embedded foundation", *Structural Engineering in the 21<sup>st</sup> Century*, ASCE, 61-65.
- Cheng, F.Y. (2001), *Matrix Analysis of Structural Dynamics: Application to Earthquake Engineering*, Marcel Dekker, Inc., New York, NY.
- Luco, J.E. (1998), "A simple model for structural control including soil-structure interaction effects", *Earthq. Eng. Struct. Dyn.*, **27**, 225-242.
- Pantelides, C.P. and Cheng, F.Y. (1990), "Optimal placement of controllers for seismic structures", *Int. J. Eng. Struct.*, **12**, 254-262.
- Smith, H.A., Wu, W.H. and Borja, R.I. (1994), "Structural control considering soil-structure interaction effects", *Earthq. Eng. Struct. Dyn.*, **23**, 609-626.
- Wolf, P. (1987), *Soil-Structure Interaction Analysis in Time Domain*, Prentice-Hall, New York.
- Zhang, X.Z., Cheng, F.Y., Jiang, H.P., Chen, G.D. and Lou, M.L. (2002), "Hybrid control realization in building structures and effectiveness comparison with MR control", *CD-ROM Proc. of the 15<sup>th</sup> ASCE Eng. Mech. Conf. (Ed. A.W. Smyth)*, New York.